JOURNAL OF SPACECRAFT AND ROCKETS
Vol. 35, No. 5, September–October 1998

Physics of Resonance in a Supersonic Forward-Facing Cavity

Dale W. Ladoon,* Steven P. Schneider,† and John D. Schmisseur‡
Purdue University, West Lafayette, Indiana 47907

An experimental study of a blunt nose with a forward-facing, cylindrical cavity was conducted in a Mach 4, quiet-flow wind tunnel. The length of the cavity was varied, whereas the diameter was fixed. A fast-response pressure transducer was located at the cavity base. Under conventional (noisy) wind-tunnel conditions, the rms pressure fluctuations were nearly 0.4% of the mean pressure. Under quiet-flow conditions, the rms fluctuations were on the order of 0.04% of the mean. A laser-perturbation system created controlled, repeatable, and localized disturbances upstream of the bow shock. These disturbances convected with the flow, impinged on the nose, and caused damped cavity oscillations. As the cavity length was increased, the resonant frequencies and the damping both decreased. The small damped oscillations present under quiet-flow conditions seem to explain the low heat transfer rates measured previously in flight. The large fluctuation levels observed in conventional wind tunnels are an artifact of the high levels of noise present there and should not be expected under typical flight conditions.

Nomenclature

A	= dimensional constant in Eqs. (2) and (3)
a_0	= speed of sound in the cavity, based on stagnation temperature
D	= diameter of cavity
f_{1n}	= primary resonant frequency, Hz
L	= depth of cavity
L^*	= axial distance from the cavity base to the mean shock position, $L + \delta$
L_{crit}	= value of L at which self-sustained oscillations may begin; Eq. (4)
M	= Mach number
m	= exponent of curve fit to measured damping; Eqs. (2) and (3)
p_{01}	= stagnation pressure in driver tube, equal to test-section stagnation pressure
p_{2t}	= mean pressure at cavity base (total pressure behind the normal shock)
p'_{2t}	= pressure fluctuations at cavity base
$p'_{2\text{rms}}$	= rms value of pressure fluctuations at cavity base
γ	= exponential damping constant [Eq. (2)], rad/s
δ	= mean shock standoff distance
ω_1	= measured primary resonant, cavity-oscillation frequency, rad/s
$\omega_{1\text{crit}}$	= value of ω_1 at which self-sustained oscillations may begin [Eq. (4)], rad/s
ω_{1n}	= theoretical primary resonant cavity-oscillation frequency [Eq. (1)], rad/s

Introduction

OPTICALLY guided interceptor missiles, cruise missiles, and self-propelled artillery that can operate in the upper supersonic to hypersonic range are of considerable military interest. The combination of low altitude and high velocity imposes a severe heat transfer environment at the stagnation region of the nose tip. A proposed passive heat transfer reduction mechanism is to locate a forward-facing cavity at the nose tip.[1–4] There is strong evidence that the heat flux at the cavity base can be as little as 2 to 10 times less than the stagnation point heat flux of a conventional convex tip.[1] The forward-facing cavity concept has been the focus of a number of recent high-speed missile programs, including the hollow-nosed active seeker program[1] and the hit-to-kill endoatmospheric strapdown seeker.[5]

The present study is concerned with blunt noses in which the cavity is located along the body axis. The forward-facing cavity scheme is depicted in Fig. 1. Design issues concerning forward-facing cavities are summarized in Ref. 6.

Background

A forward-facing cavity may be regarded as a resonance tube. The flow and heating in resonance tubes have been the subject of many experimental investigations.[7–10] However, the majority of these experiments involved the flow of a supersonic jet over a forward-facing cavity. The flow impinging on the cavity is, therefore, likely to be very noisy and not indicative of freestream flight conditions.

Experimental and numerical investigations have consistently found that the forward-facing cavity resonates and that the oscillations have a dominant frequency. This fundamental, or primary-mode, frequency is approximated from resonant tube theory as

$$\omega_{1n} = 2\pi f_{1n} = \pi a_0 / 2L^* \tag{1}$$

In Eq. (1), it is assumed that the flow velocity in the tube, or cavity, is small, so that the stagnation temperature can be used to estimate the average speed of sound.

Hopko and Strass,[11] Stallings and Burbank,[12] and others found that the stagnation point heat transfer for a hemispherical concave nose was considerably less than that of a convex hemispherical nose. Smith[13] and other investigators also observed that the bow shock oscillated at the primary-mode frequency of the cavity. For the majority of these wind-tunnel tests, the bow shock shape was stable. That is, while oscillating or at steady state, the bow shock was symmetric about the nose. When the bow shock shape was stable, the stagnation point heat transfer was on the order of 20% of that of a convex hemisphere.[11] In a few experiments, the bow shock shape was unstable. In these cases, schlieren photographs showed that the bow shock did not oscillate in a controlled manner and that it exhibited a characteristic bulge or nonsymmetrical shape.[11] The stagnation point heat transfer increased dramatically for the unstable condition.

Marquart et al.[14] and Huebner and Utreja[1,15] studied the bow shock dynamics and heat transfer of a nose piece with a slightly tapered cylindrical cavity at Mach 10. In conjunction with these studies, Sambamurthi et al.[16] performed a time-dependent, viscous, two-dimensional calculation of the flow in the cavity. Dynamic pressure measurements showed that the cavity resonated. Laser

Received Dec. 1, 1997; revision received April 17, 1998; accepted for publication April 21, 1998.

*Graduate Research Assistant, School of Aeronautics and Astronautics; currently Gas Turbine Aerodynamics Engineer, General Electric Company, Power Systems, 1 River Road, Schenectady, NY 12345. Member AIAA.

†Associate Professor, School of Aeronautics and Astronautics. Senior Member AIAA.

‡Ph.D. Student, School of Aeronautics and Astronautics; currently Aerospace Engineer, Aeronautical Sciences Division, U.S. Air Force Research Laboratory, Wright–Patterson Air Force Base, OH 45433-7005. Member AIAA.

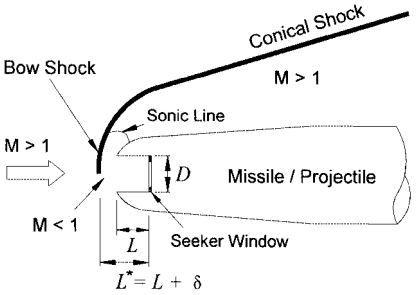

Fig. 1 Nose region of an optically guided high-speed missile with a forward-facing cavity.

interferometry measurements revealed that the bow shock oscillated at the resonant frequencies of the cavity. Because the bow shock oscillations were found to lag the base pressure oscillations, it was concluded that cavity resonance drives the bow shock oscillations.[1,15] Schlieren pictures showed that the bow shock was symmetrical about the centerline of the nose and did not come in contact with the nose during the stable oscillations.[1] However, in one experiment the bow shock exhibited a violent instability,[1] similar to that of the nonsymmetrical cases recorded by Stallings and Burbank.[12] Consistent with previous NACA/NASA experiments, the measured heat flux at the cavity base for the stable oscillations was approximately one-third that of the foremost part of the body or lip. The numerical results predicted that the oscillations damped to steady state.[16]

Yuceil and Dolling[2,17] investigated the flow and heat transfer about a forward-facing cavity in the Mach 4.9 wind tunnel at the University of Texas (UT). The models used in their experiments were blunt, hemispherical nose pieces with an axial cylindrical cavity of variable depth. In general, the cavity resonated at the primary-mode frequency, and the bow shock oscillated in a stable, symmetric manner about the nose. However, for intermediate cavity lengths, $0.4 \leq L/D \leq 0.7$, the pressure signals switched randomly between two modes of oscillation. The corresponding bow shock shapes were much like those observed in the unstable cases of Stallings and Burbank[12] and Huebner and Utreja.[1]

In conjunction with the UT experiments, Engblom et al.[4] performed viscous, time-dependent, axisymmetric numerical simulations of the flow and heat transfer in a forward-facing cavity at Mach 5. For short to moderately long cavities, artificial freestream noise was needed for the cavity to resonate. For very long cavities, resonance was obtained without freestream noise. However, this numerical result of self-sustained resonance has not been experimentally confirmed in a low-noise environment typical of flight.

Time-dependent, inviscid, axisymmetric numerical simulations for the flow about concave nose cavities at Mach 6.6 were made by Yang and Antonison[5] to simulate a transient condition due to shroud removal. Three different cavity lengths, corresponding to three different fields of view, were investigated. For the shortest cavity considered, the pressure fluctuations at the cavity base decay to a nonoscillatory steady state. The solutions for the longer cavities show that the pressure fluctuations first dampen and then oscillate at a constant, lower, amplitude. The amplitude of the oscillation was the largest for the longest cavity. This result is similar to that of Engblom et al.[4]

The measurements just cited were all conducted in conventional facilities, where the strong acoustic forcing generated by turbulent boundary layers on the wind-tunnel sidewalls results in freestream noise that is much higher than that encountered in flight.[18–21] In stark contrast, Levine[22] measured the heat transfer to a forward-facing cavity in flight. A hemispherical concave nose, or cup, was tested over a Mach number range of 2.5–7.1. Levine[22] reports that the normalized heat flux varied from 0.03–0.09 at the center point, or base, of the cup to 0.8–0.9 just inside the lip. These normalized values are based on the theoretical laminar stagnation-point heat flux for a hemispherical convex nose of the same diameter. The total heat input integrated over the surface of the nose, including the lip, was 0.58 times the theoretical value for a convex hemispherical nose with a laminar boundary layer. The general trends of low heat flux at the cavity base and increasing heat flux from the cavity base to the lip are consistent with the conventional wind-tunnel measurements. However, the magnitudes of the flight heat flux values, particularly at and near the cavity base, are considerably less than those obtained in conventional wind-tunnel tests. For instance, the center point values measured in flight were about one-fifth of those measured by Cooper et al.[23] under stable cavity flow conditions and 10 to 30 times less than those measured in conventional wind tunnels when the flow was unstable. These low heat-flux values were repeated in a second flight test but never resolved.

In an effort to examine the effects of wind-tunnel noise, Engblom et al.[24] carried out experiments in the Mach 4 Purdue University Quiet-Flow Ludwieg Tube (PQFLT). These experiments were the first high-speed, forward-facing cavity tests to be performed in a quiet-flow wind tunnel. Quiet-flow tunnels maintain laminar boundary layers on the nozzle walls, which results in test-core noise levels that are comparable to those of flight.[18,19] When the freestream noise level was small, the cavity pressure fluctuations were very small. Consequently, the large-amplitude cavity resonance observed in earlier experiments was attributed to the high characteristic noise levels of the wind tunnels used in those studies. The present quiet-flow measurements corroborate and explain the flight measurements reported by Levine.[22] Because the noise level in flight is very low, the flowfield must be nearly steady, resulting in lower heat transfer.

Experimental Apparatus

Test Facility

The present experimental study was conducted in the Mach 4 PQFLT.[19] The PQFLT is a short-duration wind tunnel with a run time of approximately 3.5 s. For atmospheric stagnation conditions in the driver tube, the corresponding unit Reynolds number in the test core is on the order of 4.5×10^4 cm^{-1}. The stagnation pressure and temperature decrease by approximately 35 and 10%, respectively, during the 3.5-s run time.[25]

Within the inviscid core flow of the nozzle is a test rhombus of uniform quiet flow. At atmosphere driver-tube conditions, the rms total pressure fluctuations in the test core flow of the PQFLT are about 0.06% (Ref. 19). These freestream noise levels are an order of magnitude less than those in conventional facilities.

Test Model and Data Acquisition

The nose-cone model used in this study, shown in Fig. 2, consisted of a 19.05-mm-diam cylinder with a 9.53-mm-radius tip. A 9.53-mm-diam hole along the axis of the nose cone served as a forward-facing cavity. The cavity length was varied by changing the position of the insert. A dynamic pressure transducer was mounted flush on the centerline of the cavity base. The transducer measured the total pressure and the fluctuations in the total pressure at the cavity base. Because the nose tip was located 21 mm downstream from the nominal onset of uniform flow in the nozzle, the diameter of uniform flow at the cavity nose is about 10.9 mm, which is greater than the cavity diameter. The freestream Mach number varies from 3.90 to 4.0 over the remaining portion of the 19.05-mm-diam nose.[19]

The output of the dynamic pressure transducer was amplified by a factor of 100 using a low-noise instrumentation amplifier. One channel was then high-pass filtered at 800 Hz and fed to an additional amplifier to provide another gain of 100 on the ac portion

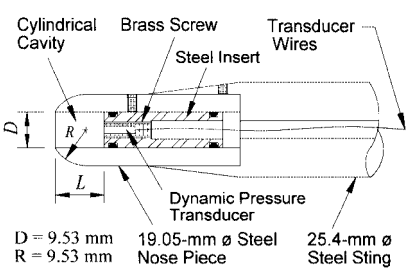

Fig. 2 Sectional view of the forward-facing cavity model.

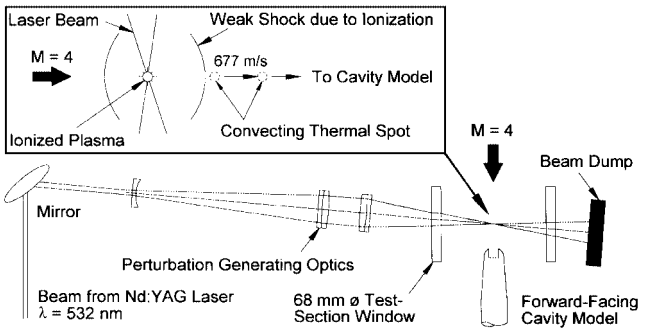

Fig. 3 Optical system for generating perturbations; inset shows the thermal spot.

of the signal. The amplified signals were acquired by an eight-bit digital oscilloscope. For the unperturbed freestream tests, continuous records were collected at a sampling frequency of 250 kHz. For the laser-perturbation tests, segmented records of 5000 or 10,000 points were acquired at 0.1-s intervals during the 3.5-s run time of the PQFLT. Sampling frequencies of 500 kHz and 5 MHz were used. Each segment was triggered by a laser pulse to consistently sample the same period with respect to a laser-generated perturbation.

Laser Perturbation System

Controlled, localized, and repeatable perturbations were produced by photoionizing a small region of the air upstream of the model bow shock using a pulsed laser.[26,27] The laser beam was focused to a point approximately 22 mm upstream of the cavity inlet. The initial disturbance, shown in the inset of Fig. 3, consists of a plasma core surrounded by a region of nonionized air driven by the shock wave produced during ionization. After the end of the laser pulse, the plasma core relaxes and remains as a region of hot recombined gas, referred to as the thermal spot. The thermal spot convects with the local velocity of the flowfield and forms the portion of the disturbance useful as a local perturbation. Hot-wire anemometer measurements show that the thermal spot is about 5 mm in diameter upon encountering the bow shock of the cavity model.[26] The peak mass-flux deficit in the heated region is roughly one-half of the freestream mass flux, plus or minus 20–30%. Thus, the resulting perturbation is large. Measurements with a later version of the laser apparatus demonstrated repeatability of the perturbation amplitude to within 2% (Ref. 27).

Experimental Results

The cavity L/D ratios used in this study ranged from 0.0 to 1.984, and all of the experiments were conducted with the model at zero-degree angle of attack. Unless stated otherwise, the PQFLT driver-tube stagnation pressure and temperature were 100 ±3 kPa and 298 ±3 K, respectively. Furthermore, the maximum fractional errors in the measured pressure fluctuations, the ratios of rms pressure fluctuations to mean pressure, and the various frequencies are 2.1%, 2.6%, and 3.4%, respectively. The fractional error is defined as the error, or uncertainty, in a quantity divided by its reported value.

Measurements Under Natural Conditions Without Laser Perturbations

With the insert flush with the nose tip, $L/D = 0.0$, the ratio of rms pressure fluctuations to stagnation pressure, $p'_{2\mathrm{rms}}/p_{2t}$, is 0.047%. Typical traces of cavity base-pressure fluctuations for various cavity lengths are shown in Fig. 4. These base-pressure fluctuations are the result of the wind-tunnel freestream noise, as modulated by the characteristic dynamic response of the cavity. Even when $L/D = 0.0$, occasional bursts or spikes are present. These bursts are generated by the residual noise in the wind tunnel. As the cavity length is increased, the cavity begins to resonate in response to these bursts. The intermittent forcing results in resonant periods followed by periods of quieter flow. Thus, the oscillations decay. The initial amplitude of these oscillations also appears to increase with cavity length. However, the degree of cavity amplification is difficult to determine because the initial forcing amplitude is not known and the oscillations often superimpose.

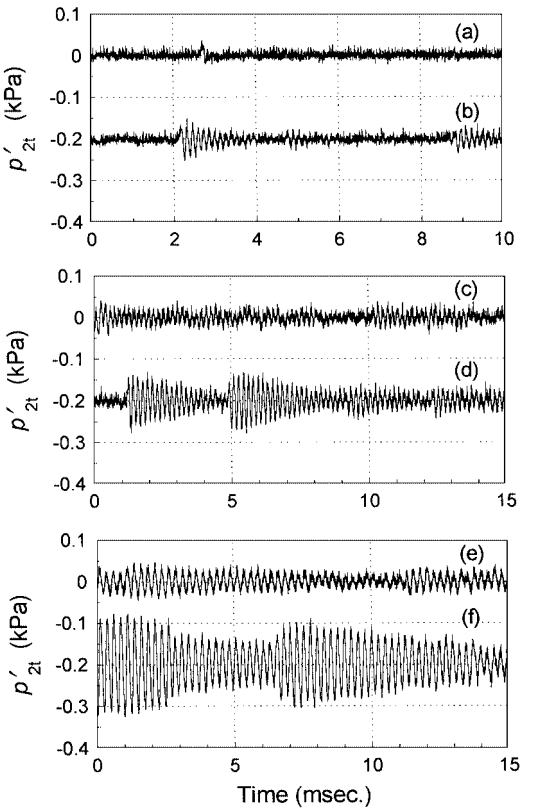

Fig. 4 Typical cavity base pressure fluctuations with no laser perturbations: *L/D* = a) 0.0, b) 0.821, c) 1.200, quieter period, d) 1.200, noisy period, e) 1.848, quieter period, and f) 1.848, noisy period. Traces in b, d, and f offset by − 0.2 kPa.

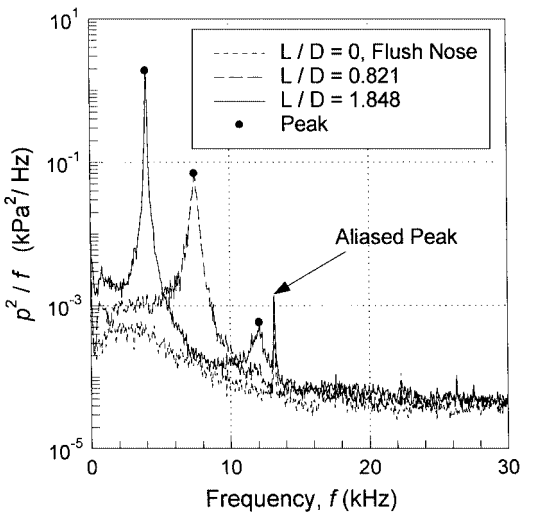

Fig. 5 Typical power spectra of the cavity base-pressure fluctuations with no laser perturbations; symbols indicate primary mode and harmonics.

Typical averaged power spectra are shown in Fig. 5. These data were acquired as a continuous record and at a sampling frequency of 250 kHz. Because the acoustic forcing field is broadband, some energy is contained at the ringing frequency of the dynamic pressure transducer, which is approximately 263.2 kHz. Consequently, an aliased peak appears at 13.2 kHz in the power spectra. In general, as the length is increased, the cavity resonates at its primary acoustical mode. The primary mode is identified as a distinct, large-amplitude peak in the power spectrum. The measured resonant frequency decreases with cavity length and agrees well with that given by Eq. (1). A harmonic also appears for deep cavities.

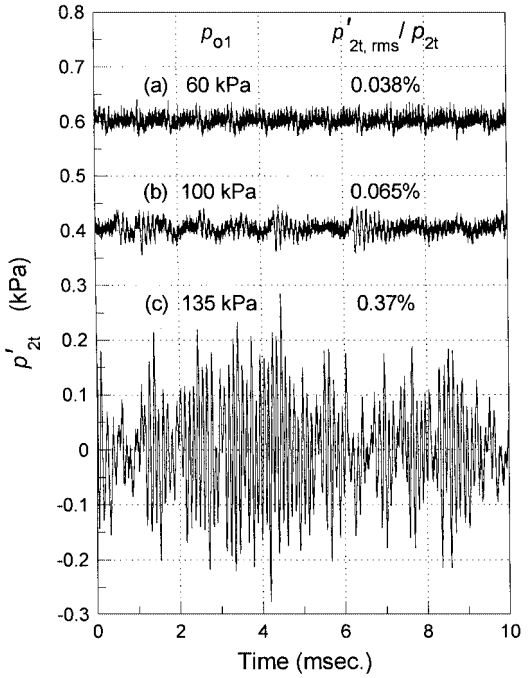

Fig. 6 Effect of freestream noise on cavity resonance for $L/D = 0.571$: a) quiet flow, b) moderately quiet flow, and c) noisy flow. Traces a and b offset by 0.4 and 0.6 kPa, respectively.

The observed periods of quiet flow agree with the computations by Engblom et al.,[4,24] which show that, in the absence of freestream noise, forward-facing cavities of moderate length do not resonate. It is clear that the forward-facing cavity is very sensitive to freestream noise. In fact, even small bursts, which are not detected at $L/D = 0.0$ or with a pitot probe, are visible as significant pressure fluctuations for deeper cavities.

Quiet flow in the PQFLT is achieved by maintaining laminar boundary layers on the test-section sidewalls upstream of the model. As the driver-tube pressure is increased, the Reynolds number increases, and the location of transition on the test-section sidewall boundary layers moves upstream. Thus, the noise level in the test core increases as the driver-tube pressure is raised. The effect of this increasing noise on the cavity resonance is shown in Fig. 6. Typical cavity base pressure fluctuations for $L/D = 0.571$ are shown for three different driver-tube pressures. The trace given in Fig. 6a is for a low driver-tube pressure where the sidewall boundary layers are laminar upstream of the model tip. The ratio of rms cavity-base pressure fluctuations to stagnation pressure, $p'_{2\text{rms}}/p_{2t}$, is 0.038%. The test core is quiet in this case. A very weak resonance, with a period of about 0.7 ms, is barely visible and may just be electronic noise. Figure 6b is a typical trace when the driver tube is at atmospheric conditions. The sidewall boundary layers begin to transition upstream of the model tip, and $p'_{2\text{rms}}/p_{2t}$ is 0.065%. Therefore, the test core is marginally quiet. The appearance of intermittent and low-amplitude resonant bursts is in response to acoustic radiation from the test-section sidewall boundary layers. The trace in Fig. 6c is for a high driver-tube pressure, where measurements have shown that the flow is noisy.[19,25] The amplitudes of the oscillations are large, and quiet periods are not present. This is the cavity response to the random and large-amplitude acoustic forcing field established by turbulent sidewall boundary layers. Note that the high-noise fluctuations shown in Fig. 6c are still more than 10 times smaller than those measured by Yuceil and Dolling[2,17] at $L/D = 0.57$ in the conventional Mach 4.9 wind tunnel at UT. Because the cavity is sensitive to freestream noise, experimental results obtained in conventional noisy wind tunnels must be used with caution.

Results Using the Laser-Generated Perturbation

This section presents cavity base-pressure data that show the response to a laser-generated hot spot produced upstream of the bow shock. The data were digitally low-pass filtered at a cutoff frequency of 200 kHz to remove the 263.2-kHz ringing frequency of the dynamic pressure transducer.[28]

Sample filtered segments, showing the cavity response to a laser spot perturbation for different cavity lengths, are given in Fig. 7. The signals in Figs. 7a–7d were sampled at a rate of 5 MHz, whereas the signals shown in Figs. 7e–7g were sampled at 500 kHz. The peak amplitudes of the pressure fluctuations are on the order of 10% of the stagnation pressure in the cavity. Note the relatively low noise level and the absence of any strong cavity resonance before the formation of a laser spot. The peak amplitudes of the laser-generated

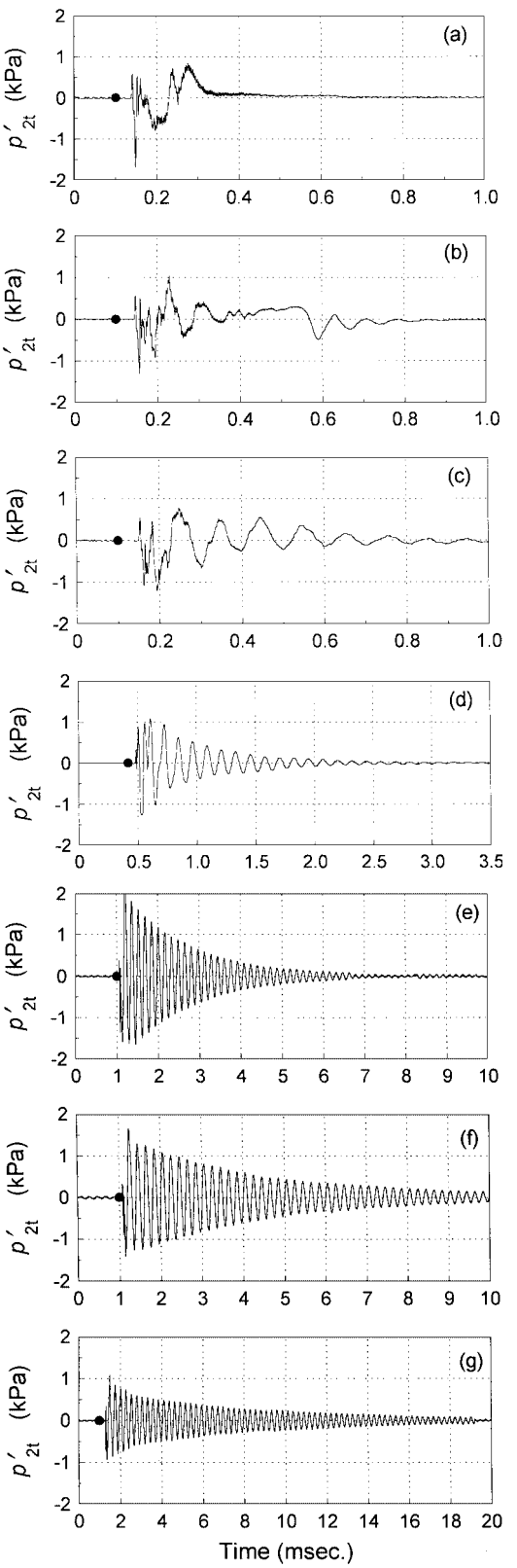

Fig. 7 Cavity base-pressure fluctuations induced by a laser spot perturbation for various cavity depths: L/D = a) 0.0 (flush nose), b) 0.272, c) 0.488, d) 0.744, e) 1.064, f) 1.429, and g) 1.984; ● denotes time of laser spot formation and $p_{2t} \approx 14$ kPa.

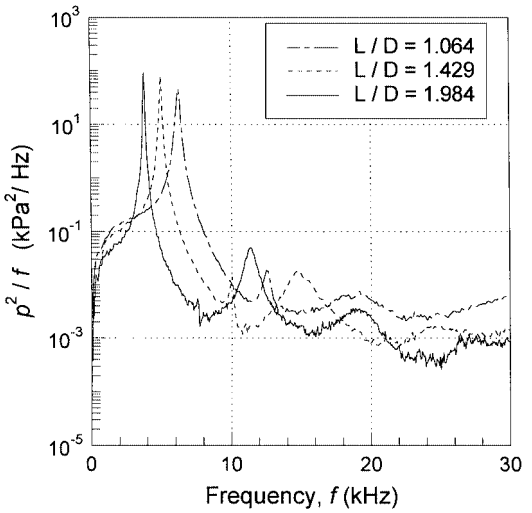

Fig. 8 Averaged power spectrum of cavity base-pressure fluctuations for various cavity depths; symbols denote primary mode and harmonics.

signals are comparable to noisy wind-tunnel data and are an order of magnitude larger than those caused by acoustic forcing from the PQFLT sidewalls under quiet-flow conditions.

Figure 7 shows that the pressure fluctuations for the flush nose case, $L/D = 0.0$, are not periodic and the effect of the laser spot quickly disappears. The cavity response in the $L/D = 0.272$ case is interesting in that the fluctuations appear to transition from a complicated state to a more simple oscillatory pattern. For L/D values of 0.488 and greater, the cavity clearly resonates in a nearly sinusoidal fashion. Moreover, these resonant signals are contained in decaying exponential envelopes. This is characteristic of an underdamped system. The decay time clearly increases with increasing cavity length. For very long cavities, successive perturbations may linearly superimpose or nonlinear interaction may occur. One would expect this to occur in noisy tunnels, where freestream perturbations are more frequent and of large amplitude.

Averaged power spectra showing the frequency content of the cavity base-pressure fluctuations for L/D ratios of 1.064, 1.429, and 1.984 are given in Fig. 8. The averaged power spectrum for a given cavity length was obtained by ensemble averaging the power spectral densities calculated from each data segment. In general, 35 segments were collected for each wind-tunnel test, and the only distinguishable peaks in the spectra were observed at frequencies less than 50 kHz.[28] For L/D ratios less than 0.488, the frequency content is largely broadband, and no clear peaks are evident. The absence of clear peaks is to be expected because the pressure signals in Fig. 7 do not exhibit a simple harmonic pattern for these cases. For cavity L/D ratios of 0.488 and greater, where the cavity resonates in an apparently one-dimensional fashion, distinct peaks appear. In Fig. 8, the lowest peak frequency corresponds to the fundamental, or primary, resonant frequency of the cavity. Subsequent peaks at higher frequencies are cavity harmonics. Interestingly, the first two harmonics for $L/D = 1.064$ and 1.429 are consecutive multiples of two and three times the primary frequency, whereas the first two harmonics for $L/D = 1.984$ are odd multiples of three and five times the primary frequency.

The primary mode is clearly the dominant frequency. As the cavity length increases, the resonant frequencies decrease. This trend is consistent with Eq. (1). Other investigators have also observed similar resonant behavior in forward-facing cavities.[1,2,4] As the cavity length is increased, the energy contained in the primary and harmonic frequencies seems to increase relative to that of the rest of the spectrum.

Because the resonant pressure fluctuations decay with time, it is the damped resonant frequencies that are measured. Damped and modulated oscillations have also been observed in other forward-facing cavity experiments.[1,15,17] A plot of the theoretical primary-mode frequency [Eq. (1)] as a function of the measured primary-mode frequency is given in Fig. 9. For the forward-facing cavity, one expects the mean shock standoff distance to be greater

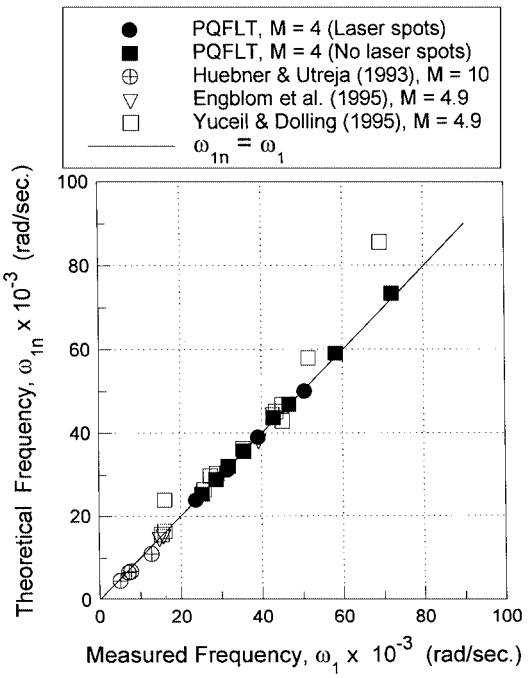

Fig. 9 Comparison of measured primary-mode frequency with theoretical natural frequency for different cavity-flow experiments.

than that of a spherical nose and less than that of a flat face nose. Because the shock standoff distance was not measured in this study, it was estimated as the arithmetic average of that given by Billig's correlation for sphere-cones [Eq. (5.37) in Ref. 29] and the flat-face cylinder data given in Fig. 4.15 of Ref. 30. Figure 9 shows that data from a wide variety of experiments collapse onto the theoretical curve reasonably well. This demonstrates that Eq. (1) predicts the primary resonant frequency of the forward-facing cavity rather well. Note that only Huebner and Utreja[1,15] measured the mean shock standoff distance.

Comparisons to Flight Data

The low base-pressure fluctuations present under quiet-tunnel conditions combine with the obviously damped perturbed-flow measurements to show that the fluctuations in the cavity will be small under the low-noise conditions typical of flight. The present measurements therefore provide an explanation for the flight data of Levine.[22] The low-noise environment typically encountered in flight results in low heat transfer levels because the freestream perturbations are small and the cavity oscillations are damped. The large fluctuations, higher heat fluxes, and high optical distortion observed in conventional wind tunnels appear to be spurious effects of the characteristically high freestream noise levels of these facilities.

Cavity Damping and Stability

As shown in Fig. 7, the pressure signals for L/D ratios of 0.488 and greater decay exponentially. Decaying exponential envelopes were least squares fitted to the peaks of these resonant signals. Typical curve fit envelopes are shown in Fig. 10. Because the power spectra show that the primary-mode frequency dominates, the exponential damping constant was expressed as

$$\gamma/2 = A\omega_1^m \tag{2}$$

where the curve fit values are $A = 1.0273 \times 10^{-12}$ and $m = 3.227$. Note that A is a dimensional constant. Using this relation, one need specify only the damped resonant frequency of the cavity to evaluate the damping constant. Because the resonant frequency is inversely proportional to the cavity length, the damping constant $\gamma/2$ decreases with cavity length L. Although the decaying signals in this study indicate that the cavity is stable, the degree of damping decreases with increasing cavity length. This decreased damping

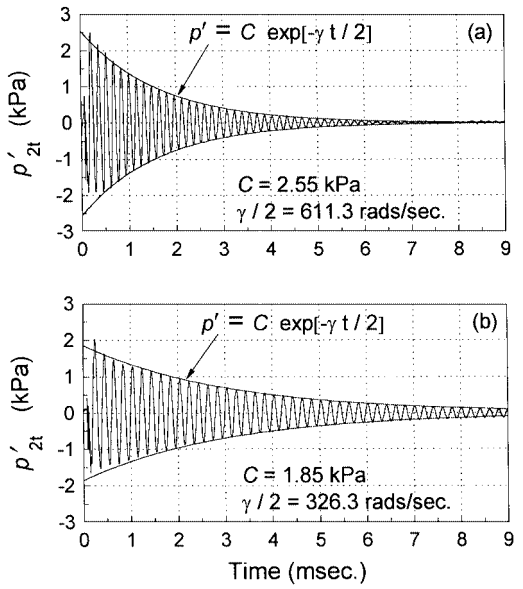

Fig. 10 Typical decaying, exponential-envelope curve fit to the measured cavity-base pressure fluctuations: *L/D* = a) 1.064 and b) 1.429.

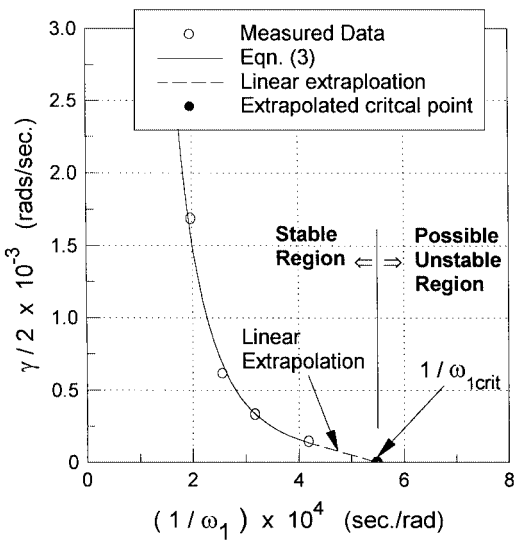

Fig. 11 Variation of damping constant with measured primary mode frequency.

suggests that for very long cavities little or no damping may be present. The damping, or attenuation, of the cavity pressure fluctuations can be attributed to viscous losses, heat conduction losses, delays in attaining thermodynamic equilibrium, and losses associated with acoustic radiation from the mouth of the cavity.[31] The primary damping mechanism seems to be acoustic radiation from the cavity mouth and the resulting propagation of acoustic waves in the subsonic region between the mouth and the bow shock.[28]

Consistent with the present experimental findings, the cavity base-pressure fluctuations in Yang and Antonison's numerical simulations appear to decay exponentially.[5] However, for short cavities their calculations show that the fluctuations damp to a steady state, whereas for long cavities the fluctuations first decay exponentially and then oscillate at a constant, lower amplitude. Thus, they predict that for long cavities an unsteady oscillatory flowfield is sustained. Similarly, numerical simulations[4,24] have predicted that for very long cavities an unstable or self-sustained condition may exist in which the cavity will resonate without the presence of freestream noise. To date, these deep-cavity results have not been experimentally confirmed in a quiet-flow facility.

Given that damping decreases with increasing cavity length, Eq. (2) may be used to estimate the cavity length at which undamped oscillations or self-sustained resonance may occur for the

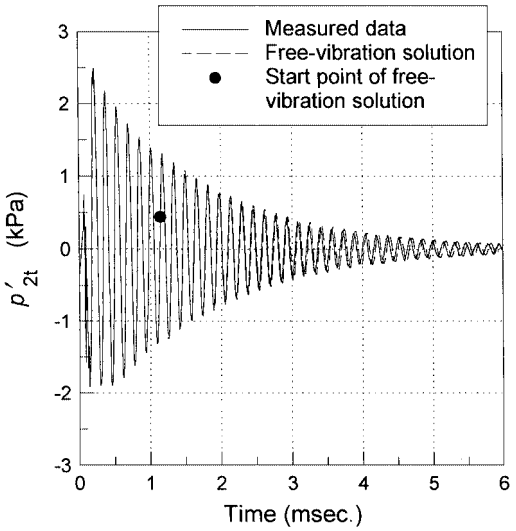

Fig. 12 Comparison of free-vibration solution with measured data for *L/D* = 1.064.

model and conditions used in this study. For this purpose, Eq. (2) can be written in a more convenient form as

$$\gamma/2 = A(1/\omega_1)^{-m} \tag{3}$$

The experimental data are shown together with the curve fit [Eq. (3)] in Fig. 11. To estimate a critical frequency at which self-sustained, or unstable, oscillations may occur, Eq. (3) was linearly extrapolated from the last data point, $L/D = 1.984$, to $\gamma/2 = 0$. Using Eq. (1), the corresponding cavity length-to-diameter ratio L_{crit}/D is

$$\frac{L_{\text{crit}}}{D} = \frac{\pi a_0}{2D\omega_{1\text{crit}}} - \frac{\delta}{D} \tag{4}$$

For the data presented in this study, $\omega_{1\text{crit}} \approx 18{,}177$ rad/s, $a_0 = 343$ m/s, $D = 9.53$ mm, and $\delta \approx 3.7$ mm. From Eq. (4), the critical cavity length-to-diameter ratio L_{crit}/D is approximately 2.7. Thus, for L/D values greater than this value, the pressure oscillations may be unstable. Further experiments are needed to confirm this extrapolation.

Model of Cavity Response

For L/D values greater than 0.488, the cavity base pressure signals are nearly sinusoidal and are contained in a decaying exponential envelope. Furthermore, the corresponding power spectra show that the majority of the signal energy is in the primary mode of oscillation. Therefore, it seems reasonable to model the cavity base-pressure fluctuations as a second-order linear system closely analogous to a single-degree-of-freedom, spring, mass, and viscously damped mechanical oscillator. The details of such a model are given in Ref. 28, and a sample comparison between the resulting free-vibration solution and the experimental data is shown in Fig. 12. In general, the one-dimensional, free-vibration solution predicts the cavity response reasonably well.[28]

Conclusions

Measurements of the pressure fluctuations in a forward-facing cavity were performed in a Mach 4 quiet-flow wind tunnel. Freestream perturbations induced resonant oscillations in the cavity for L/D values greater than 0.488. The cavity was found to be very sensitive to freestream noise. Even very weak freestream disturbances that are normally too small to be detected are amplified to measurable levels by the cavity. Amplification appears to increase with cavity length. When the cavity resonates, the majority of the signal energy is contained in the primary mode of the oscillation. Harmonics are present, however, and become stronger when the cavity length is increased.

Repeatable freestream disturbances were generated by a laser system. These controlled disturbances were used to determine the stability characteristics of the cavity flow. For L/D values greater than

0.488, the cavity base pressure fluctuations decay exponentially, and the amount of damping decreases as the cavity length is increased. The forward-facing cavity flowfield and the bow shock are weakly damped resonant oscillators because the oscillations decay to a nonoscillatory steady state. Damping constants were evaluated from the experimental data.

These quiet-tunnel measurements appear to explain the flight data. The large fluctuations, high heat fluxes, and high optical distortion observed in conventional wind tunnels are spurious effects of the high freestream-noise levels present in these facilities. In the flight data, the freestream noise was low, the cavity oscillations must have therefore been small, and this most likely caused the lower heat fluxes measured by Levine.

Acknowledgments

The equipment used in this study was purchased with funds from the Air Force Office of Scientific Research under Grant F49620-94-1-0067 (monitored by L. Sakell), a gift from The Boeing Company, and a gift in memory of K. H. Hobbie. The authors would like to thank Don Bower, Madeline Chadwell, and Joe Zachary for their quality craftsmanship.

References

[1]Huebner, L. D., and Utreja, L. R., "Mach 10 Bow-Shock Behavior of a Forward-Facing Nose Cavity," *Journal of Spacecraft and Rockets*, Vol. 30, No. 3, 1993, pp. 291–297.

[2]Yuceil, K. B., and Dolling, D. S., "Nose Cavity Effects on Blunt Body Pressure and Temperatures at Mach 5," *Journal of Thermophysics and Heat Transfer*, Vol. 9, No. 4, 1995, pp. 612–619.

[3]Shui, V., Reeves, B., and Thyson, N., "Multiple Aperture Window and Seeker Concepts for Endo KEW Applications," AIAA Paper 92-2806, May 1992.

[4]Engblom, W. A., Yuceil, B., Goldstein, D. B., and Dolling, D. S., "Hypersonic Forward-Facing Cavity Flow: An Experimental and Numerical Study," AIAA Paper 95-0293, Jan. 1995.

[5]Yang, H. Q., and Antonison, M., "Unsteady Flowfield over a Forward-Looking Endoatmospheric Hit-to-Kill Interceptor," *Journal of Spacecraft and Rockets*, Vol. 32, No. 3, 1995, pp. 440–444.

[6]Shui, V., and Reeves, B., "Uncooled Aperture for Endoatmospheric Optical Seeker," AIAA Paper 93-2673, June 1993.

[7]Powell, A., and Smith, T. J., "Experiments Concerning the Hartmann Whistle," Dept. of Engineering, Rept. 64-42, Univ. of California, Los Angeles, CA, Sept. 1964.

[8]Sarohia, V., and Back, L. H., "Experimental Investigation of Flow and Heating in a Resonance Tube," *Journal of Fluid Mechanics*, Vol. 94, 1979, pp. 649–672.

[9]Ericsson, L. E., and Reding, J. P., "Unsteady Aerodynamic Flow Field Analysis of the Space Shuttle Configuration. Part III: Unsteady Aerodynamics of Bodies with Concave Nose Geometries," Lockheed Missiles and Space Co., Inc., LMSC-D057194, April 1976 (NASA citation 76N25330).

[10]Vrebalovich, T., "Resonance Tubes in a Supersonic Flow Field," Jet Propulsion Lab., California Inst. of Technology, TR 32-378, Pasadena, CA, July 1962 (NASA citation 63N13447).

[11]Hopko, R. N., and Strass, K. H., "Some Experimental Heating Data on Convex and Concave Hemispherical Nose Shapes and Hemispherical Depressions on a 30° Blunted Nose Cone," NACA RM-L58a17a, March 1958.

[12]Stallings, R. L., and Burbank, P. B., "Heat-Transfer and Pressure Measurements on a Concave-Nose Cylinder for a Mach Number Range of 2.49 to 4.44," NASA TM-X-221, Oct. 1959.

[13]Smith, F. M., "A Wind-Tunnel Investigation of Effects of Nose Bluntness, Face Shape, and Afterbody Length on the Aerodynamic Characteristics of Bodies of Revolution at Mach Numbers of 2.37, 2.98, and 3.90," NASA TM-X-230, April 1960.

[14]Marquart, E. J., Grubb, J. B., and Utreja, L. R., "Bow-Shock Dynamics of a Forward-Facing Nose Cavity," AIAA Paper 87-2709, Oct. 1987.

[15]Huebner, L. D., and Utreja, L. R., "Experimental Flowfield Measurements of a Nose Cavity Configuration," Society of Automotive Engineers, Paper 871880, Warrendale, PA, Oct. 1987.

[16]Sambamurthi, J. K., Huebner, L. D., and Utreja, L. R., "Hypersonic Flow Over a Cone with Nose Cavity," AIAA Paper 87-1193, June 1987.

[17]Yuceil, K. B., and Dolling, D. S., "IR Imaging and Shock Visualization of Flow over a Blunt Body with Nose Cavity," AIAA Paper 96-0232, Jan. 1996.

[18]Beckwith, I. E., and Miller, C. G., "Aero-Thermodynamics in High-Speed Wind Tunnels at NASA Langley," *Annual Review of Fluid Mechanics*, Vol. 22, 1990, pp. 419–439.

[19]Schneider, S. P., and Haven, C. E., "Quiet-Flow Ludwieg Tube for High-Speed Transition Research," *AIAA Journal*, Vol. 33, No. 4, 1995, pp. 688–693.

[20]Laufer, J., "Aerodynamic Noise in Supersonic Wind Tunnels," *Journal of the Aerospace Sciences*, Vol. 28, No. 9, 1961, pp. 685–692.

[21]Pate, S. R., and Schueler, C. J., "Radiated Aerodynamic Noise Effects on Boundary-Layer Transition in Supersonic and Hypersonic Wind Tunnels," *AIAA Journal*, Vol. 7, No. 3, 1969, pp. 450–457.

[22]Levine, J., "Additional Heat-Transfer Measurements Obtained in Free Flight on a Hemispherical Concave Nose at Mach Numbers up to 7.1," NASA TM-X-466, April 1961.

[23]Cooper, M., Beckwith, I. E., Jones, J. J., and Gallagher, J. J., "Heat-Transfer Measurements on a Concave Nose Shape with Unsteady-Flow Effects at Mach Numbers of 1.98 and 4.95," NACA RM-L58D25a, July 1958.

[24]Engblom, W. A., Goldstein, D. B., Ladoon, D., and Schneider, S. P., "Fluid Dynamics of Hypersonic Forward-Facing Cavity Flow," *Journal of Spacecraft and Rockets*, Vol. 34, No. 4, 1997, pp. 437–444.

[25]Schneider, S. P., Collicott, S. H., Schmisseur, J. D., Ladoon, D., Randall, L. A., Munro, T. R., and Salyer, T. R., "Laminar-Turbulent Transition Research in the Purdue Quiet-Flow Ludwieg Tube," AIAA Paper 96-2191, June 1996.

[26]Schmisseur, J. D., "Receptivity of the Boundary Layer on a Mach-4 Elliptic Cone to Laser-Generated Localized Freestream Perturbations," Ph.D. Dissertation, School of Aeronautics and Astronautics, Purdue Univ., West Lafayette, IN, Dec. 1997.

[27]Schmisseur, J. D., Schneider, S. P., and Collicott, S. H., "Receptivity of the Mach 4 Boundary Layer on an Elliptic Cone to Laser-Generated Localized Freestream Perturbations," AIAA Paper 98-0532, Jan. 1998.

[28]Ladoon, D. W., Schmisseur, J. D., and Schneider, S. P., "Laser-Induced Resonance in a Forward-Facing Cavity at Mach 4," AIAA Paper 97-0339, Jan. 1997.

[29]Anderson, J. D., *Hypersonic and High Temperature Gas Dynamics*, McGraw–Hill, New York, 1989.

[30]Liepmann, H. W., and Roshko, A., *Elements of Gasdynamics*, Wiley, New York, 1957.

[31]Kinsler, L. E., and Frey, A. R., *Fundamentals of Acoustics*, 2nd ed., Wiley, New York, 1962.

J. R. Maus
Associate Editor